Donor-Acceptor Layer Formation and Lattice Site Preference in the Solid: The $CaBe_2Ge_2$ Structure

Chong Zheng and Roald Hoffmann*

Contribution from the Department of Chemistry and Materials Science Center, Cornell University, Ithaca, New York 14853. *Received October 11, 1985*

Abstract: The $Be_2Ge_2^{2-}$ part of the $CaBe_2Ge_2$ structural type is built up of two distinguishable, isomeric layers, the Be and Ge occupying distinct sublattices within one layer and switching their positions in the next layer. A consequence of this differential site occupation is a difference in the dispersions of the Be–Ge bonding and antibonding bands. We define a more dispersive lattice site as being one that engenders more overlap between equivalent sites. In general, if a lattice is made up of several sublattices which differ in dispersivity, and if the lattices may be occupied by atoms of different electronegativity, then depending on the degree of band filling the more electronegative atom will enter or avoid the more dispersive sites. For low band filling the more electronegative atom should enter the more dispersive sites, and for high band filling the more electronegative atoms should be found in the less dispersive sublattice. When Ge is at this site in one layer in $CaBe_2Ge_2$ the occupied band is wide and has a higher ϵ_f, transferring electron density to the other layer to form a dielectric material. The high dispersion in the occupied band (mostly of Ge states) is a destabilizing factor within one layer but a better supporter of interaction with an inverted layer in a donor–acceptor mode. The electronegativity and orbital contraction provide tuning for the intra- and interlayer interaction. As the orbitals of the X element become more diffuse when X goes down in the Periodic table, the interlayer interaction favoring the $CaBe_2Ge_2$ structure wins out.

The design of organic or inorganic materials with specific desirable physical, especially electronic, properties has benefited much from ideas of molecular donor–acceptor pair proximity or charge transfer. Examples of such inspirations include a proposed molecular diode of donor–acceptor molecules connected by σ bond chain molecules,[1] organic ferromagnets of donor–acceptor pairs with the donor (or acceptor) molecule having a stable triplet ground state,[2] and chemical systems built up by donors and acceptors connected by light absorbers capable of photosynthesis,[3] to mention a few. The donor–acceptor concept, when generalized to extended two- or three-dimensional systems, may provide us with a tool to understand bonding in the solid state. We will see in this paper that this is the case for the $CaBe_2Ge_2$ structure, where the donor and acceptor are two-dimensional layers.

The $CaBe_2Ge_2$ Structure

The $CaBe_2Ge_2$ structure,[4] **1**, is a variation of another very common phase, $ThCr_2Si_2$,[5] **2**. The latter phase, into which more

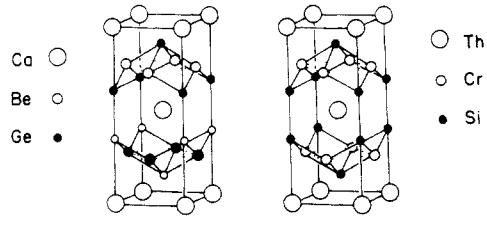

1 **2**

than 400 compounds crystallize,[6] consists of layers which are common to many other structures. These layers can be thought of as being "split" from yet another very common structure, CsCl, according to **3**.[7] This "splitting" process is imaginary, but it may

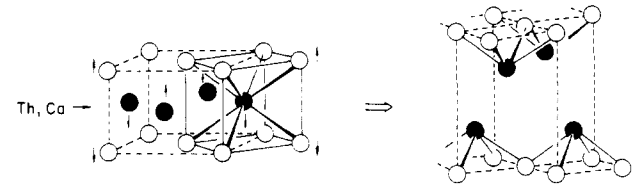

3

be more than that; a line of development in solid-state chemistry is the tailoring of three-dimensional solids into lower dimensional ones and modifying the interfaces between lower dimensional layers to produce desired physical properties.[8] The "splitting out" viewpoint may also provide us with a correlation between the high occurrence of the $ThCr_2Si_2$ structure and that of the CsCl structure.

The layers which build up the AB_2X_2 compounds crystallizing in the $ThCr_2Si_2$ structure have the following feature: the element B forms a square lattice, the element X sits alternately above and below the square lattice holes, **4**. In such an arrangement, the

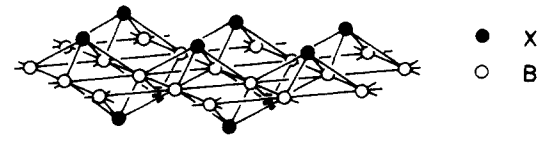

4

element B is at the center of the tetrahedron formed by the X element, and the BX_4 tetrahedron propagates into a two-dimensional layer by sharing four of its six edges, **5**.

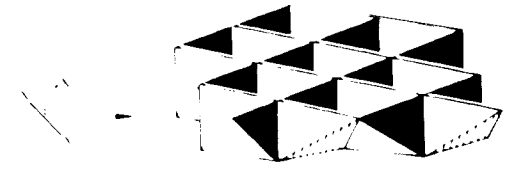

5

(1) (a) Aviram, A. *Biotech 83*; Northwood: U.K., 1983; pp 695–704. (b) Aviram, A.; Ratner, M. A. *Chem. Phys. Lett.* **1974**, *29*, 277.
(2) (a) Breslow, R.; Jaun, B.; Kluttz, R. Q.; Xia, C.-Z. *Tetrahedron* **1982**, *38*, 863–867. (b) Breslow, R. *Pure Appl. Chem.* **1982**, *54*, 927–938.
(3) Wrighton, M. S. *Comments Inorg. Chem.* **1985**, *4*, 269.
(4) Eisenmann, B.; May, N.; Müller, W.; Schäfer, H. *Z. Naturforsch., B: Anorg. Chem., Org. Chem.* **1972**, *27*, 1155–1157.
(5) Ban, Z.; Sikirica, M. *Acta Crystallogr.* **1965**, *18*, 594.
(6) (a) Marchand, R.; Jeitschko, W. *J. Solid State Chem.* **1978**, *24*, 351. Jeitschko, W.; Jaberg, B. *Ibid.* **1980**, *35*, 312. Hofmann, W. K.; Jeitschko, W. *Ibid.* **1984**, *51*, 152. (b) Parthé, E.; Chabot, B.; Braun, H. F.; Engel, N. *Acta Crystallogr., Sect. B: Struct. Sci.* **1983**, *39*, 588. (c) Pearson, W. B. *J. Solid State Chem.* **1985**, *56*, 278. (d) Hulliger, F. *Helv. Phys. Acta* **1985**, *58* 216–225.
(7) Wells, A. F. *Structural Inorganic Chemistry*, 4th ed.; Clarendon Press: Oxford, 1975; p 218.
(8) Rao, C. N. R.; Thomas, J. M. *Acc. Chem. Res.* **1985**, *18*, 113.

0002-7863/86/1508-3078$01.50/0 © 1986 American Chemical Society

There are two kinds of B_2X_2 layers in the $CaBe_2Ge_2$ structure: one is the same as that in the $ThCr_2Si_2$ structure **4** and other is **6**. In **6** the arrangement is different: it is now the X element which forms the square lattice, with the B element sitting alternately

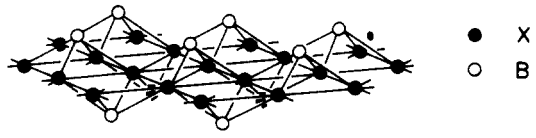

6

above and below the square lattice holes. The two layers are not identical but isomeric. To a first approximation, we may consider Ca merely as a two-electron donor ($Ca \rightarrow Ca^{2+} + 2e^-$) and ignore the interlayer interaction for the time being. The three-dimensional net may be thought of as consisting of two-dimensional layers, which we call **A** and **D**, as in **7**. The **A** and **D** notation anticipates what will turn out to be an important electronic property of these layers.

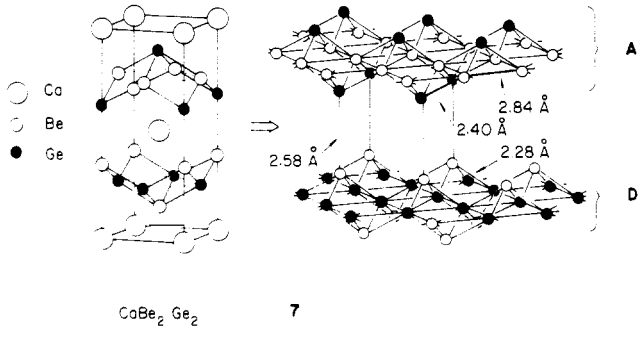

7

Band Dispersion and Its Correlation to Lattice Sites

On going from a discrete molecule to a solid of infinite extent, the energy levels become a continuum indexed by a continuous variable k (k is the wave vector, wave node counter, or symmetry label). As in the molecular case, the energy separation between the lowest level (most bonding) and the highest level (most antibonding)—the band width or band dispersion—is determined by the interaction between atoms. In the case of weak interaction, where the interatomic distance is large, the separation between lowest and highest level is small and the energy band has small dispersion. On the contrary, if the interatomic distance is short and the interaction is strong, there will be a big dispersion. The two situations are contrasted in **8**.

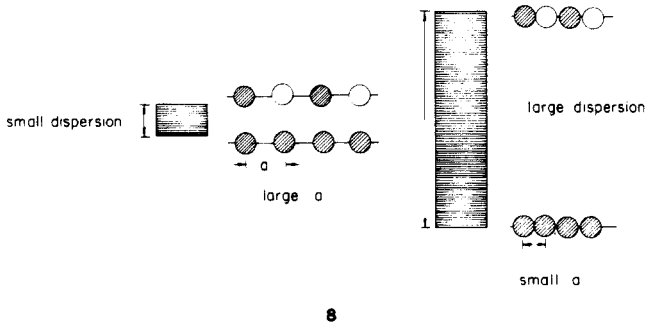

8

In a crystal there might exist several *nonequivalent* lattice sites. We call a specific lattice site more *dispersive* if the separation between the *equivalent* sites of that particular kind is smaller than that of other sites. An example is the two-dimensional layer in $ThCr_2Si_2$ or $CaBe_2Ge_2$ structure, **9**, where we emphasize the different lattice sites by deleting the connections between them. Both layers, I and II, are square lattices. But in layer I the distance between the lattice sites is shorter than that in layer II. Thus the lattice sites in layer I (which are all equivalent) are more dispersive.

The lattice sites in layer I are twice as dense as in layer II. So when all the sites in layer I and two sheets of layer II are occupied, the ratio of the number of atoms of site I to those at site II is 1:1,

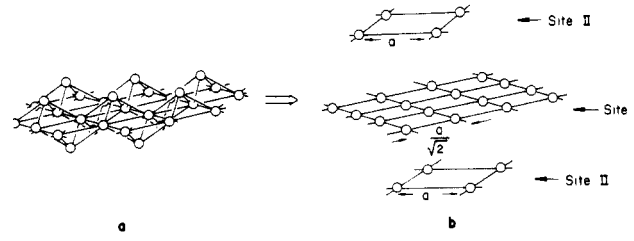

9

as in the case of Cr_2Si_2 or Be_2Ge_2 in $ThCr_2Si_2$ or $CaBe_2Ge_2$.

The dispersivity of lattice sites will be reflected in the width of the energy bands, which in turn will affect the energetics of the solids. Given atoms of different electronegativities, the question arises as how to arrange them among different lattice sites so to minimize the lattice energy. This is the so-called "coloring" problem,[9] one aspect of which we will discuss later in this paper. We will now study the donor–acceptor layer formation in the $CaBe_2Ge_2$ lattice.

Donor–Acceptor Layer Formation in $CaBe_2Ge_2$ Structures

The layers **A**, **4**, and **D**, **6**, in $CaBe_2Ge_2$ have the stoichiometry $Be_2Ge_2^{2-}$ or $BeGe^-$. One might think of $BeGe^-$ as the building "bricks" of the layers. **10** and **11** emphasize the diatomic $BeGe^-$ units in the layers **A** and **D**. In these layers each $BeGe^-$ monomer

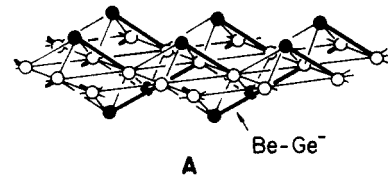

A

10

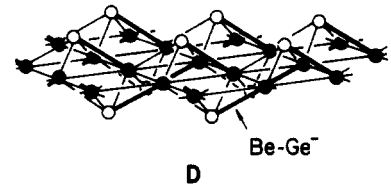

D

11

pointing "up" is surrounded by 4 others pointing "down" in a square-planar coordination geometry. In **A** the Be end of the Be–Ge^- monomer resides in lattice site I; in **D** it is the Ge and which occupies lattice site I.

The typical interatomic distances for a tetrahedral arrangement (Be at the center of Ge_4 tetrahedron in **A** and Ge at the center of Be_4 in **D**) are shown in **7**. The Be–Ge distances are the shortest and presumably the strongest in the structure. So it makes sense to focus on the Be–Ge unit as the primary building block, turning on supplemental Be···Be, Ge···Ge, and interlayer Be···Ge interactions as perturbations.

A schematic portrayal of the orbital interaction in a Be–Ge^-

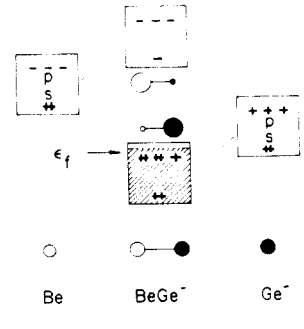

12

(9) Burdett, J. K.; Lee, S.; McLarnan, T. J. *J. Am. Chem. Soc.* **1985**, *107*, 3083–3089.

monomer is given in **12**. The more electronegative Ge, orbitals lower in energy, interacts with Be. The germanium's one s and three p orbitals are pushed down in energy. Correspondingly, the Be orbitals are lifted up by this interaction. Five electrons from Ge^- and two from Be occupy 7 of the 8 available states in the lower block, mostly of Ge character. The lower block is $^7/_8$ filled and the Fermi level ϵ_f (or HOMO) separates the filled and the $^1/_8$ unfilled states in the lower block.

On constructing a two-dimensional layer from the Be–Ge^- monomers we have two choices: one is to put the Be side in the more dispersive site (central layer I in **9b**). This will result in a bigger dispersion in the upper block of the Be–Ge^- orbital levels in **12** since that block is more localized on Be, and it is the Be's which are put more in contact by this choice of lattice site. The other choice is to place the Ge end into the more dispersive site, resulting in a bigger dispersion in the lower block in **12**, mostly of Ge character. The two situations are contrasted in **13**. Please remember that these are schematic drawings. We will soon make them more precise (and complicated) through band calculations.

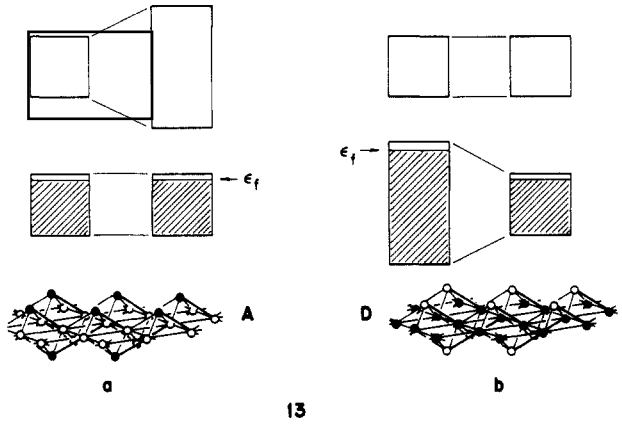

13

We now proceed to the three-dimensional lattice. When layers **A** and **D** are stacked together to form the $Be_2Ge_2^{2-}$ framework of the $CaBe_2Ge_2$ structure, the Fermi levels of both layers should equalize. To accomplish this, electron transfer from layers **D** to **A** should occur, resulting in formation of a dielectric material, shown schematically in **14**. Our calculation, to be discussed below, gives a charge transfer of 0.6 e^- from **D** to **A** per unit cell or 0.3 e^- per Be–Ge^- monomer.

It is worthwhile to note that some AB_2X_2 compounds where **B** is a transition-metal element crystallize in two phases. The low-temperature form is the $ThCr_2Si_2$ structure consisting of only **A** layers. The high-temperature phase is the $CaBe_2Ge_2$ structure built up from both **A** and **D** layers. One can obtain the $CaBe_2Ge_2$ form by quenching from high temperature and study its superconducting behavior. The first example was $LaIr_2Si_2$, reported by Braun, Engel, and Parthé.[10] Recently this was reported for YIr_2Si_2.[11] Shelton et al.[12] have measured the superconducting temperatures for both of these compounds, as well as for a series of AB_2X_2 compounds crystallizing either in the $ThCr_2Si_2$ or in the $CaBe_2Ge_2$ structure, where A = La, Y, Th, U; B = Ru, Rh, Pd, Os, Ir, Pt; and X = Si, Ge. From this study it seems that the $CaBe_2Ge_2$ phase is more likely to be a superconductor. Possibly relevant to this is that there has been some speculation that excitonic superconductors, in which the conducting electron pairs are in one metallic layer mediated by excitons of another dielectric layer, would have higher T_c.[13] Some researchers recently also suggested nonphononic superconductivity; one of the materials is $CeCu_2Si_2$ crystallizing in $ThCr_2Si_2$ structure.[14] So there are good reasons to examine the structure, both geometric and electronic, of these fascinating materials.

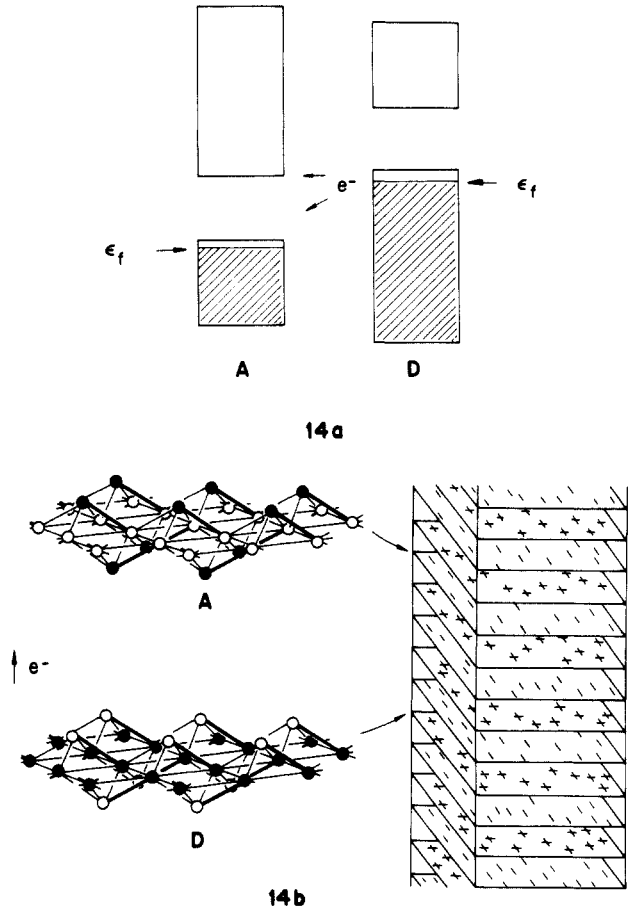

We have discussed qualitatively the donor–acceptor layer formation. Now let us look at some of the detailed features of their electronic structure obtained from our extended-Hückel calculations.

The Electronic Structure of $CaBe_2Ge_2$

The starting point is a diatomic $BeGe^-$ monomer. Figure 1 is an interaction diagram for that. In the lower block of the resulting $BeGe^-$ levels there are four orbitals: the lowest 1σ and 2σ are the Be and Ge's orbitals and sp_z (z is chosen along the Be–Ge^- axis) hybrid bonding combinations; then come the two degenerate π orbitals. These lower orbitals have bigger coefficients on Ge and thus the electrons occupying them concentrate on Ge. The LUMO, 3σ, as well as the other orbitals above it, has bigger coefficients on Be. We will construct the approximate band structures from these molecular orbitals. The geometry of the layers has been described: each Be–Ge^- monomer sticking up is surrounded by four other nearest Be–Ge^- monomers pointing down in the layer. In layer **A** it is the Be side which resides in the central square lattice site; in layer **D** the Ge side of the monomer takes over this position. Let us begin the construction for layer **A**. We will embed each Be–Ge^- MO into the lattice and determine the nature of the dispersion of the band developed from the MO by changing the phase relation between Be–Ge^- monomer and its four nearest neighbor monomers.

15 shows this process for the lowest Be–Ge^- MO, 1σ, in layer **A**. A rule to determine the phase relation is the following: the Be–Ge^- monomer 1 (pointing up) in **15** is related by a glide plane (reflection in the central square lattice pland and translation along the direction indicated by the arrow) to another nearest neighbor 2. When this symmetry operation is performed, if the phase is the same we have in-phase propagation (corresponding to the Γ

(10) Braun, H. F.; Engel, N.; Parthé, E. *Phys. Rev. B* **1983**, *28*, 1389.
(11) Higashi, I.; Lejay, P.; Chevalier, B.; Étourneau, J.; Hagenmuller, P. *Rev. Chim. Minér.* **1984**, *21*, 239.
(12) Shelton, R. N.; Braun, H. F.; Musik, E. *Solid State Commun.* **1984**, *52*, 797–799.
(13) *High-Temperature Superconductivity*; Ginzburg, V. L., Kirzhnits, D. A., Eds.; Consultants Bureau; New York, 1982.
(14) (a) A leading review is the following: Stewart, G. R. *Rev. Mod. Phys.* **1984**, *56*, 755 and also the references on theoretical work cited therein. (b) A nonphononic mechanism was proposed for other compounds, e.g., for the A15 phase: Kataoka, M. *J. Phys. Soc. Jpn.* **1985**, *54*, 29.

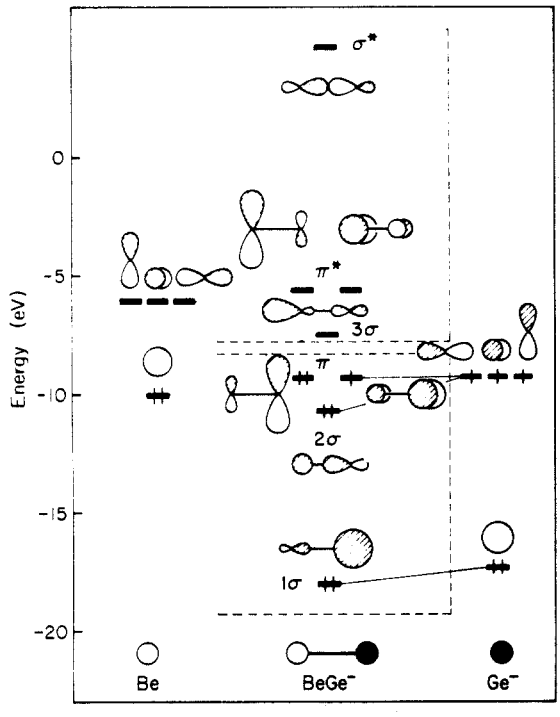

Figure 1. An interaction diagram for Be–Ge$^-$ formed from Be and Ge$^-$.

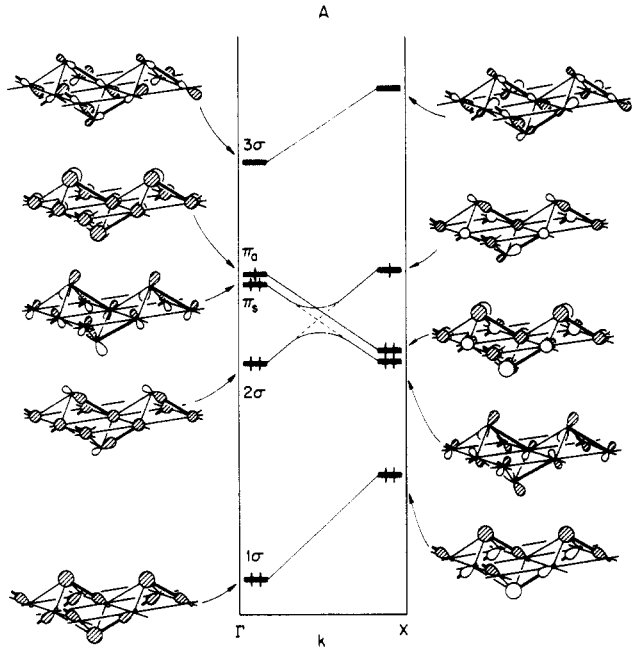

Figure 2. Schematic band structures for $Be_2Ge_2^{2-}$ layer **A**, plotted from Γ(0,0) to X($^1/_2$,0).

point in the Brillouin zone), otherwise it is out-of-phase propagation (zone boundary).[15]

Thus **15** corresponds to the Γ point and **16** to the zone boundary, X. As indicated by the arrow in **16** the orbital at the X point has strong inter-unit-cell antibonding character, thus the band developing from 1σ should rise up in energy when going from Γ to X.

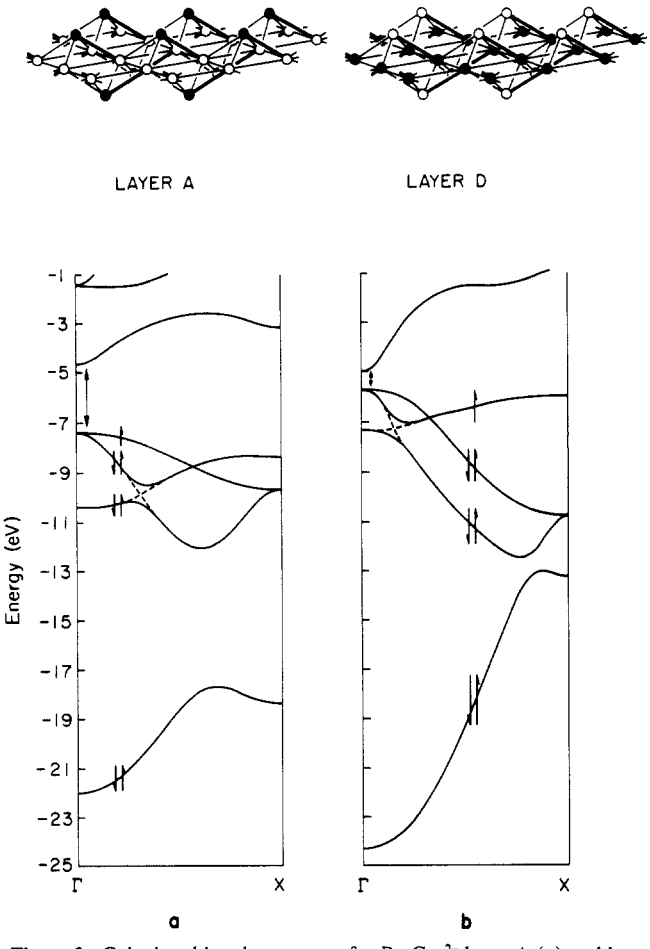

Figure 3. Calculated band structures for $Be_2Ge_2^{2-}$ layer **A** (a) and layer **D** (b).

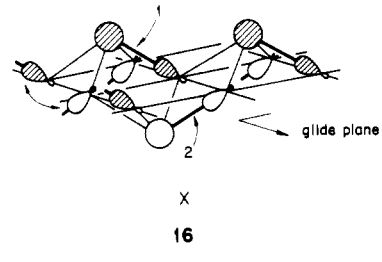

16

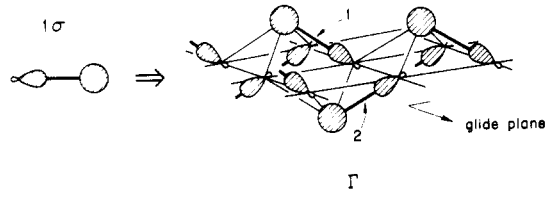

15

We can proceed to work out the approximate band structure derived from other MO's, as Figure 2 shows. Since all the σ-type orbitals have the same topology, the bands generated from them should behave similarly: they should go up in energy from Γ to X, as the 1σ band does. The π orbitals go down in energy along the same line in the Brillouin zone for the following reason.

The two orbitals π_a and π_s are plotted in **17** and **18** in a view from above the square lattice. At the Γ point, where monomer 1 does not change phase when mapped into monomer 2 by the glide plane, the antibonding character indicated by the arrows in **17a** pushes the π_a orbital high above the same orbital at the X point. For the π_s orbital there are 2 nearest bonding (solid

(15) In the Bloch sum $\hat{P}\phi$ where $\hat{P}$ is the projector $\hat{P} = \Sigma_R e^{i\mathbf{k}\cdot\mathbf{R}}\hat{T}_R$ and ϕ an arbitrary function the symmetry operation $\hat{T}_R$ can be something other than translation, as long as $\{\hat{T}_R\}$ is Abelian and represented by $\{e^{i\mathbf{k}\cdot\mathbf{R}}\}$. In our case $\hat{T}_R$ is the glide plane (or the twofold screw axis) and **k** is no longer planewave but contains an angular part. There have been some applications of this idea, where the asymmetric unit is chosen as the unit cell to simplify calculations for biological systems: (a) Imamura, I. *J. Chem. Phys.* **1970**, *52*, 3168. (b) Fujita, H.; Imamura, I. *Ibid.* **1970**, *53*, 4555. (c) Suhai, S. *Biopolymers* **1974**, *13*, 1731. (d) *Quantum Chemistry of Polymers—Solid State Aspects*; Ladik, J., Andrē, J.-M., Eds.; D. Reidel Publishing Company: Dordrecht, Holland, 1984; pp 337–359. For solid-state applications see: (e) Hughbanks, T.; Hoffmann, R. *J. Am. Chem. Soc.* **1983**, *105*, 3528.

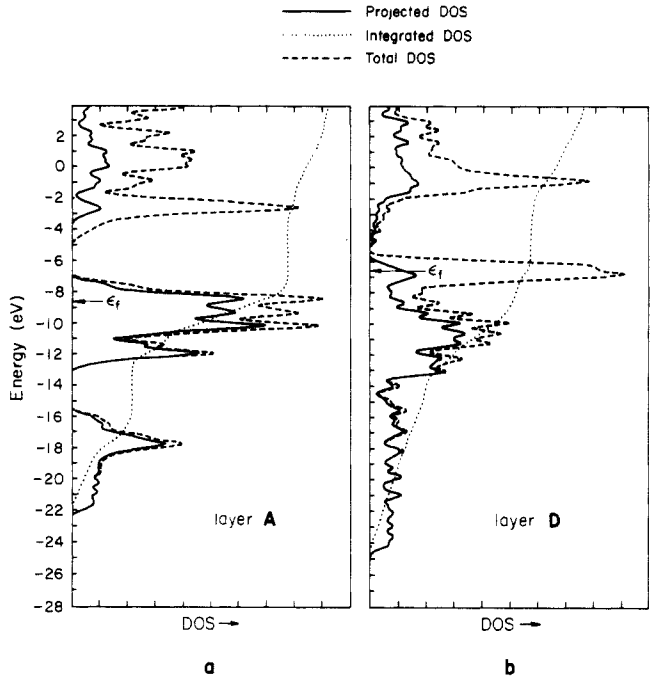

Figure 4. Calculated total density of states (dashed lines) and the contributions from the Be–Ge⁻ bonding MO's (solid lines) for $Be_2Ge_2^{2-}$ layer **A** (a) and layer **D** (b). The dotted lines indicate the integrated Be–Ge⁻ bonding states.

arrow) and 4 next nearest antibonding (dotted arrow) interactions. It turns out that the antibonding feature wins out. Thus the two bands π_a and π_s drop down in energy from Γ to X. Moreover, π_a is antisymmetric with respect to the plane **m** perpendicular to the paper and indicated in **17** and **18**. But π_s is symmetric, as are all the other σ orbitals. Hence π_s has an avoided crossing with one of the σ-type bands.

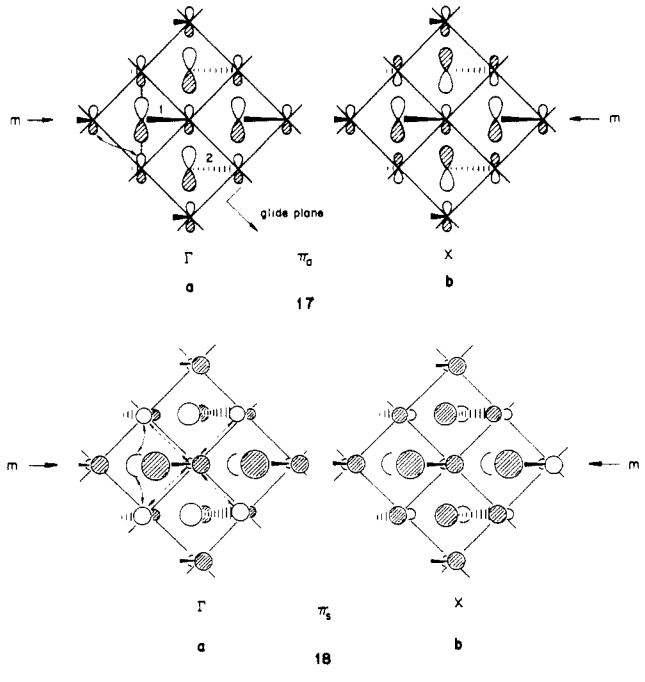

The reader may wonder why there are only four low-lying bands (mainly Ge) in Figure 2, whereas the true unit cells contain two BeGe units and so eight bands (two s and six p) would be expected. What we have done in the preceding discussion and will continue to do in the remainder of the paper is to utilize maximally the symmetry available, and in particular the glide plane symmetry.[15] The complete band structure may be obtained by "folding back" areas and lines of the larger Brillouin zone for one BeGe per

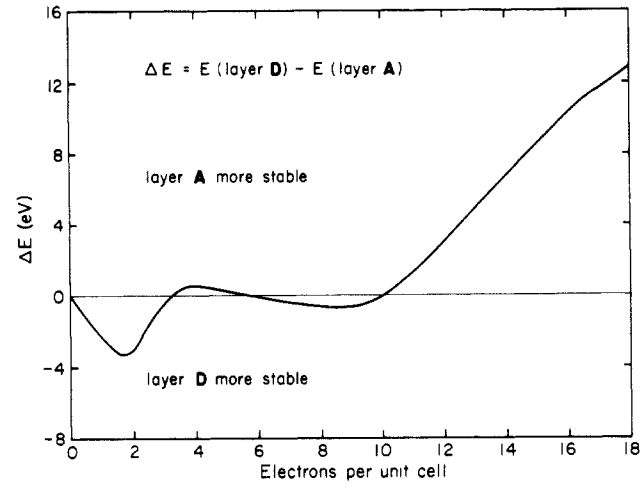

Figure 5. Total energy difference between Be_2Ge_2 layer **D** and layer **A** as a function of electron count in the unit cell.

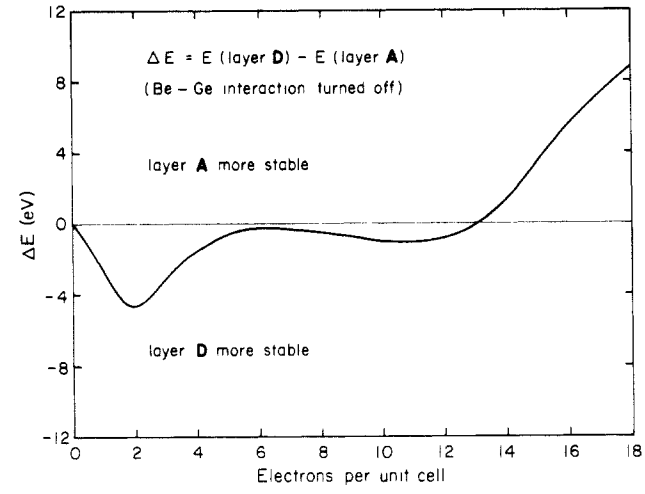

Figure 6. Same as in Figure 5, except that the Be–Ge interaction is turned off here.

asymmetric unit that we use here into the smaller zone for the true Be_2Ge_2 unit cell.

Figure 3a shows the calculated band structures for the $Be_2Ge_2^{2-}$ layer **A**. The lowest 5 bands have the appropriate features that we indicated schematically in Figure 2: 3 σ-type bands rise up and 2 π-type bands drop down, with an avoided crossing between one of the π bands and a σ band. The electron occupation in BeGe⁻ is such that there are 7 electrons per BeGe, or 3.5 filled bands.

The same analysis applies to layer **D**. However, when we put the Ge side of the Be–Ge⁻ unit into the central square lattice there will be more overlap between these sites for those occupied MO's which have bigger coefficients on Ge. The situation for 1σ is shown in **19**, in contrast to **15** and **16**. The bigger lobe of 1σ resides in the central square lattice, enhancing the difference in energy between the Γ and X points. The same is true for all other

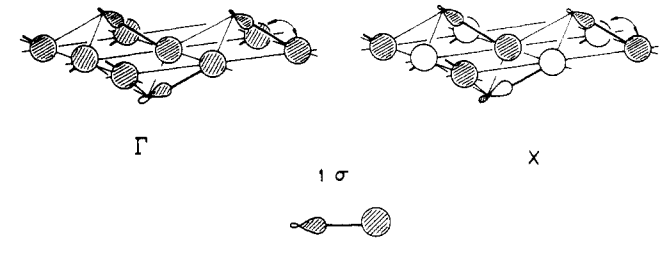

19

occupied orbitals: the bonding and the antibonding extremes within each band will both be enhanced. What should happen is indicated schematically in **20**, which reproduces Figure 2 and

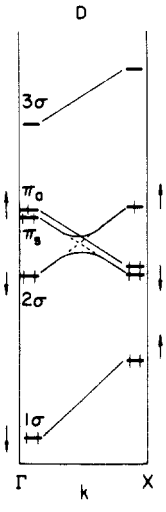

20

indicates by arrows the change expected upon putting Ge in the more dispersive site. The most important consequence of this should be a reduction in the band gap.

The calculated band structures for layer **D** are shown in Figure 3b. Indeed the band gap is decreased. *What we have is a layered material in which there is a periodic variation of the band gap in the lattice.* Another well-known material with band gap variation is the solid-state superlattice,[16] **21**, which has many

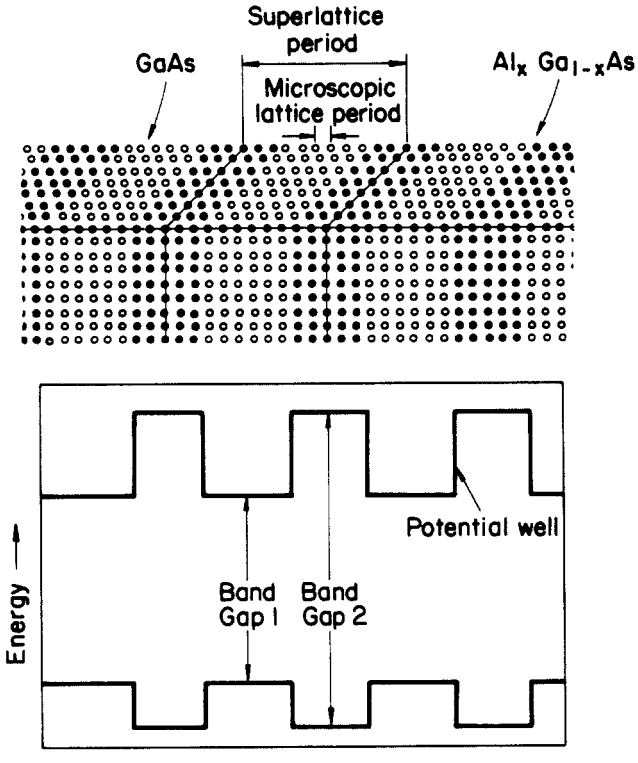

21

interesting physical properties. However, the period of the band gap variation in the superlattice is in the order of 10^2 Å. A smaller value would increase the tunneling between different layers and reduce the effective band gap difference.[16] Furthermore, the charge transfer from donor to acceptor layer by this tunneling effect leaves the valence band in the narrow-gap layer positively charged. Correspondingly, there are less electrons thermally

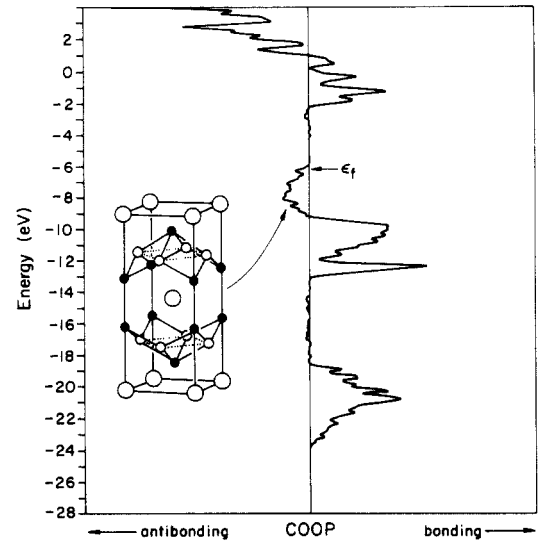

Figure 7. Crystal orbital overlap population for the interlayer Ge–Ge bond in the **A** + **A** stacked $ThCr_2Si_2$ structure.

excited into the conduction band. The valence band shifts to a lower energy scale and the conduction band to a higher one, just as a positively charged atom has a bigger (magnitude) ionization potential and a negatively charged one a smaller one (compare H^- with H, for example). Thus the band gap in the donor layer becomes bigger. For the same reason the band gap in the acceptor layer gets smaller. The band gap difference is reduced until the electron transfer is inhibited by the electric field induced by this charge transfer. This is shown schematically in **22**.[17]

22

A strategy to reduce the interlayer tunneling is to have big cations intercalated between layers **A** and **D** in $CaBe_2Ge_2$-type compounds. Could organometallic or organic cations serve here?

Enhancing the dispersion difference in the occupied bands (see **13**) should increase the ϵ_f difference which in turn leads to a greater band gap difference. A combination of small atom B and big atom X with large electronegativity difference should be a good choice for this purpose, as long as other chemical requirements are satisfied.

However, solid-state chemistry provides us with more diversified opportunities. For example, two B_2X_2 layers can be condensed into one,[18] **23**; the layer composition can be changed,[19] **24**; and the interlayer distance may be increased by inserting other layers,[20]

(16) A good introduction is the following: (a) Döhler, G. H. *Sci. Am.* **1983**, *249* (No. 5), 144. Reviews on compositional superlattices: (b) Esaki, L. *Proceedings of a NATO Advanced Study Institute on Molecular Beam Epitaxy and Heterostructures*; Erice, Italy, March 7–19, 1983 (Dordrecht, Netherlands: Martinus Nijhoff, 1985); pp 1–36. On doping superlattices: (c) Ploog, K. *Ibid.*, pp 533–74. A new type, the effective-mass superlattice, was recently proposed: (d) Sasaki, A. *Phys. Rev. B* **1984**, *30*, 7016–7020.

(17) An example is the following: (a) Hundharsen, M.; Ley, L.; Carius, R. *Phys. Rev. Lett.* **1984**, *53*, 1598. See also: (b) Chen, I. *Phys. Rev. B* **1985** *32*, 879, 885.

(18) Klepp, K.; Boller, H.; Völlenkle, H. *Monatsch. Chem.* **1980**, *111*, 727–733.

(19) (a) Dörrscheidt, W.; Schäfer, H. *J. Less-Common Metals* **1978**, *58*, 209–216; **1980**, *70*, P1–P10.

(20) (a) Brechtel, E.; Cordier, G.; Schäfer, H. *Z. Naturforsch., B: Anorg. Chem., Org. Chem.* **1979**, *34*, 251–255; **1980**, *35*, 1–3; *J. Less-Common Metals* **1981**, *79*, 131–138. (b) Cordier, G.; Eisenmann, B.; Schäfer, H. *Z. Anorg. Allg. Chem.* **1976**, *426*, 205–214. (c) Cordier, G.; Schäfer, H. *Z. Naturforsch., B: Anorg. Chem., Org. Chem.* **1976**, *32*, 383–386. (d) May, N.; Schäfer, H. *Ibid.* **1974**, *29*, 20. (e) Dorrscheidt, W.; Savelsberg, G.; Stöhr, J.; Schäfer, H. *J. Less-Common Metals* **1982**, *83*, 269–278.

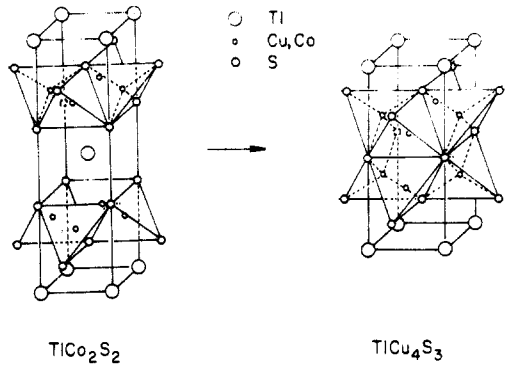

23

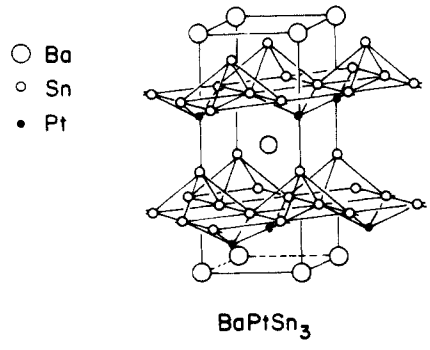

24

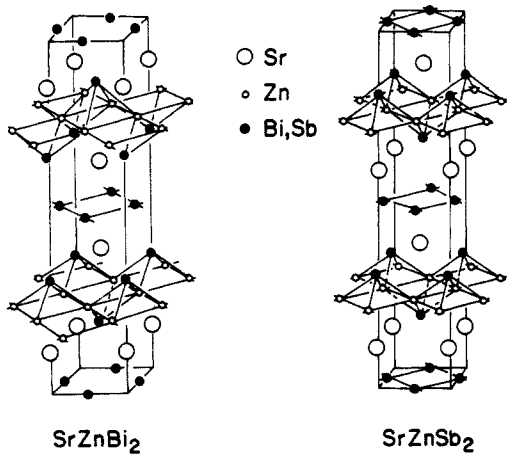

25

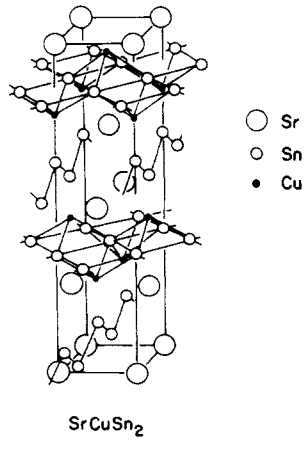

26

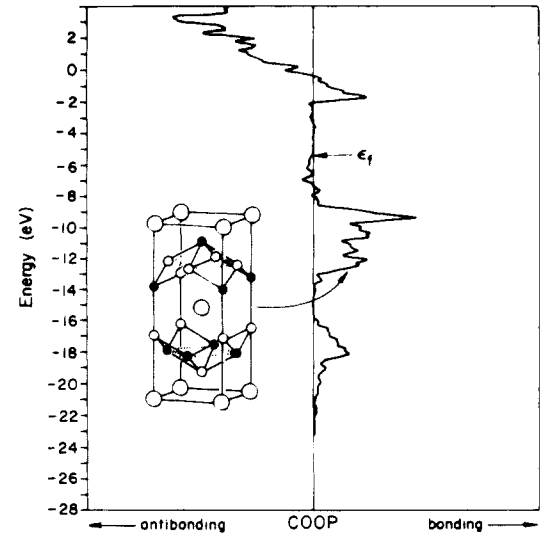

Figure 8. Crystal orbital overlap population for the interlayer Be–Ge bond in the **A** + **D** stacked $CaBe_2Ge_2$ structure.

25 and **26**. It will not be a surprise if some of the interesting physical phenomena unique to a two-dimensional system[21] are observed in one or another of these layered compounds.[22]

Site Preference

As indicated in **13**, layer **D** has a higher Fermi energy and if isolated would be unstable relative to layer **A**. Figure 4 shows the calculated density of states (DOS) and the contributions to it of the Be-Ge monomer bonding states (the 4 lowest orbitals in Figure 1), for both layers. The higher dispersion in the filled states (in **13b**) pushes more Be–Ge bonding states above the Fermi level in layer **D** than in layer **A**. This decomposition, the position of the Fermi level, and the calculated total energy per unit cell of the two layers all indicate greater stability for layer **A**.

However, site preference is a function of band filling. As **13** indicates, the same factor that favors the more dispersive site for the less electronegative atom for $CaBe_2Ge_2$ would operate in the opposite direction were the band less than half filled.

To put it another way: for situations such as that occurring in $CaBe_2Ge_2$ and summarized schematically in the approximate band structure of **13** (a lattice is made up of several sublattices which differ in dispersivity), for low band fillings bonding will be maximized and dispersivity favored while for high band fillings dispersivity is destabilizing. This is nothing but the usual contrast between two-electron two-orbital stabilization vs. four-electron two-orbital destabilization that we encounter repeatedly as a determinant of structure and reactivity in discrete molecules.[23]

Returning to our specific $CaBe_2Ge_2$ case, we plot the energy difference between layers **A** and **D** as a function of electron count in Figure 5. There indeed layer **D** is more stable for very low electron filling, but for the normal filling of 14 electrons per unit cell, layer **A** is more stable than layer **D** by about 6.7 eV per unit cell (2 Be–Ge units) from our extended-Hückel calculation.

It should be noted that this conclusion as to the effect of band filling and dispersivity on site preference is quite independent of the interaction of the two nonequivalent lattices with each other. If the distance between Be and Ge layers is stretched over a large range, still curves such as Figure 5 are obtained. Figure 6 is such an illustration, where we have deleted the Be–Ge interaction in the 2-dimensional layer.

In many other examples, molecular and extended structures, the site preference is well-determined for a given electron count and two elements of different electronegativity, **27**–**30**.[24] A

(21) Ando, T.; Fowler, A. B.; Stern, F. *Rev. Mod. Phys.* **1982**, *54*, 437.
(22) In their first proposal of a superlattice, Esaki and Tsu also considered SiC which has a superlattice period a = 15–53 Å, but the potential amplitude may be too small: Esaki, L.; Tsu, R. *IBM J. Res. Dev.* **1970**, *14*, 61–65.
(23) (a) Salem, L. *Chem. Br.* **1969**, *5*, 449. (b) Salem, L. *J. Am. Chem. Soc.* **1968**, *90*, 543.

particularly interesting result is that of Burdett et al., who applied the moment method to the coloring problem and concluded that

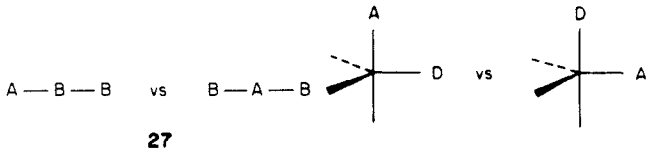

27 28

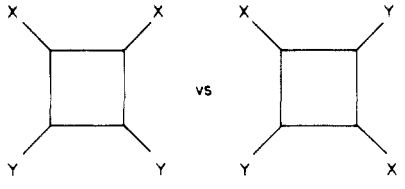

29

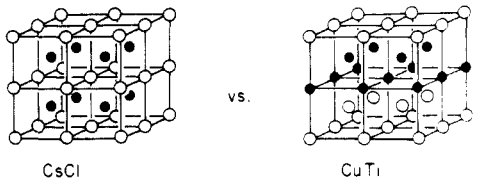

30

for a half-fitted band the structure in which the A–B interaction is maximized is favored over that where the A–A and B–B interactions are maximized, when the fourth moment μ_4 dominates.[9]

While these site preferences are highly illuminating, we still need to understand the $CaBe_2Ge_2$ structure, and this is approached in the next section.

Interlayer Interaction in $CaBe_2Ge_2$

The site preference arguments of the previous section allow us to predict the sorting of atoms of different electronegativity among nonequivalent sites of a B_2X_2 layer. And so we can understand the preferred isomerism in $ThCr_2Si_2$ structures. But in $CaBe_2Ge_2$ Be and Ge occupy both the more dispersive and the less dispersive sites. We have shown that layer **D** is unstable against layer **A**, thus the extra stabilization in the real structure must come from interlayer interaction. We would like to understand this.

31 shows the schematic interlayer interactions when the **A** layers are stacked to form the $ThCr_2Si_2$ structure, **2**. The Ge's on the outside of the layers interact with each other and the lower block in the band structures will become wider, the upper part being of Ge–Ge antibonding character. Figure 7 shows the COOP curves[25] for this Ge–Ge bond, and the antibonding features immediately below the Fermi level are there as we expected.

Perhaps a word is in order about the crystal orbital overlap population (COOP) curves.[25] These are really overlap population weighted densities of states and gauge the bonding capabilities of all the energy levels in a given energy interval. They are the solid-state analogue of an overlap population, with positive values indicating bonding and negative ones antibonding.

The general feature of X···X pairing in the $ThCr_2Si_2$ structure type is an important aspect of bonding in this class. We refer the reader to a detailed discussion of the problem elsewhere.[26a] We will refer to this A···A stacking here in less detail, only as an alternative to the $CaBe_2Ge_2$ structure.

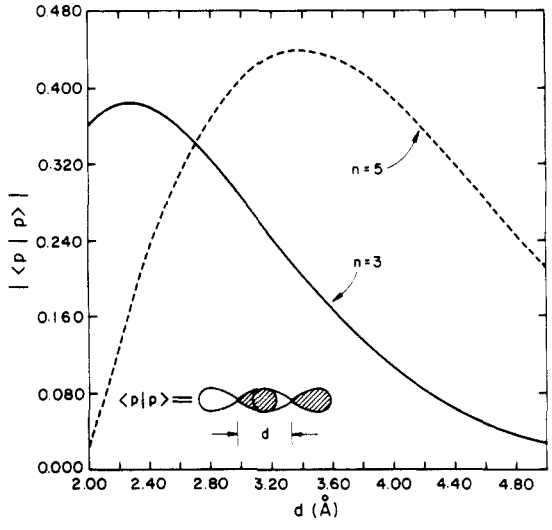

Figure 9. Absolute values of the overlaps between two p orbitals as a function of the separation. Solid line: $n = 3$. Dashed line: $n = 5$.

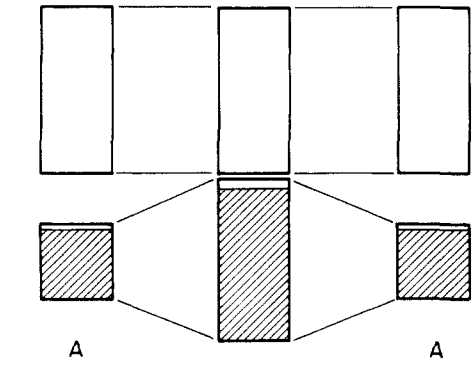

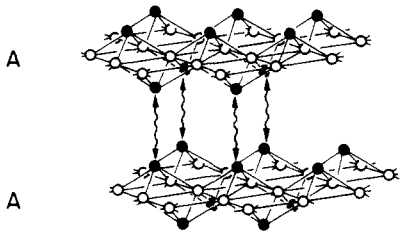

31

The situation where the **A** and **D** layers are stacked together to form the $CaBe_2Ge_2$ structure is depicted in **32**. The empty upper block representing Be in layer **D** interacts with the filled lower block characterizing Ge in layer **A**, resulting in a typical stabilizing donor–acceptor interaction scheme. The donor states in **A** are stabilized and the acceptor states in **D** are pushed up in energy. But the lower block in **D** and the upper block in **A** remain unchanged, since Ge of **D** and Be of **A** are in the central layer and out of interaction distance. Figure 8 shows the COOP curve for this Be–Ge bond responsible for the **A**–**D** interlayer interaction. It is of bonding character below the Fermi level, as **32** suggested.

Thus there are two factors competing: the small dispersion in the lower block in **13** favors layer **A** by itself and **A**–**A** stacking, while the donor–acceptor interaction in **32** favors the simultaneous

(24) (a) Gimarc, B. M. *Molecular Structure and Bonding*; Academic Press: New York, 1979; p 153. (b) Hoffmann, R.; Howell, J. M.; Muetterties, E. L. *J. Am. Chem. Soc.* **1972**, *94*, 3047. Rossi, A. R.; Hoffmann, R. *Inorg. Chem.* **1975**, *14*, 365. (c) Hoffmann, R. *Chem. Commun.* **1969**, 240. (d) Burdett, J. K. *Prog. Solid State Chem.* **1984**, *15*, 173.

(25) Some other applications of the COOP curves may be found in the following: (a) Wijeyesekera, S. D.; Hoffmann, R. *Organometallics* **1984**, *3*, 949. (b) Kertesz, M.; Hoffmann, R. *J. Am. Chem. Soc.* **1984**, *106*, 3453. (c) Saillard, J.-Y.; Hoffmann, R. *Ibid.* **1984**, *106*, 2006.

(26) (a) Hoffmann, R.; Zheng, C. *J. Phys. Chem.*, **1985**. (b) Fischer, H.-O.; Schuster, H.-U. *Z. Anorg. Allg. Chem.* **1982**, *491*, 119.

(27) Schäfer, H., to be published.

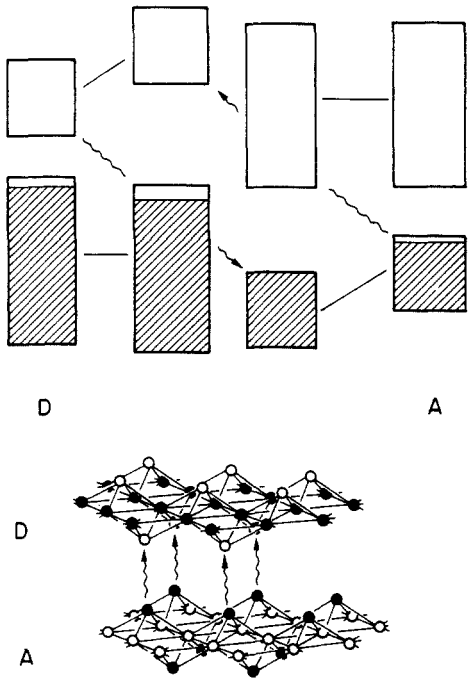

32

presence and bonding of A and D layers. Which effect dominates depends on the electronegativity and orbital diffuseness difference between B and X in AB_2X_2 compounds. Our extended-Hückel calculations for $CaBe_2Ge_2$ (really with Si parameters for Ge, see Appendix) do not capture this balance correctly—they prefer the A + A stacking to A + D. Nevertheless, both bonding components mentioned above are present; so we are prompted to think in greater depth about the factors influencing the relative magnitude of the band dispersion and donor–acceptor interactions. Some structure systematics point to an important role of the position in the Periodic table of the B and X elements.

The energy difference between layers A and D arises from the inequality between the lower block band dispersions in **13**. Thus reducing the degree of this inequality should decrease the energy difference between A and D layers. The dispersion inequality in turn derives from the difference of overlaps within a given sublattice. What we should have for this purpose is a set of orbitals which have bigger overlaps between site II's in **9** (4.02 Å apart for $CaBe_2Ge_2$) than the overlaps between site I's (2.84 Å for $CaBe_2Ge_2$). This is not easy to arrange, for most overlaps do not scale in this way. The only candidate that comes to mind is a p–p σ overlap of type **33**. For every p orbital there is a range of distances over which while $d_1 > d_2$, $S_{pp}(d_1) > S_{pp}(d_2)$. The range in question depends on the contraction (exponent) of the orbitals,

$d_1 > d_2$

$|S_{pp}(d_1)| > |S_{pp}(d_2)|$

33

the more diffuse the orbital the greater the distance of maximum overlap. Figure 9 shows the effect of varying the principal quantum number while keeping the effective Z constant in a Slater orbital with $Z_{eff} = 1.38$. For $n = 5$ the maximum overlap occurs around 3.6 Å and is greater at 4.0 Å than at 2.8 Å. This is a good situation for a $CaBe_2Ge_2$ structure with a lattice constant $a \sim 4$ Å. Figure 10 shows the DOS of A and D layers and the B–X bonding contribution for $n = 5$. Compared with Figure 4, the

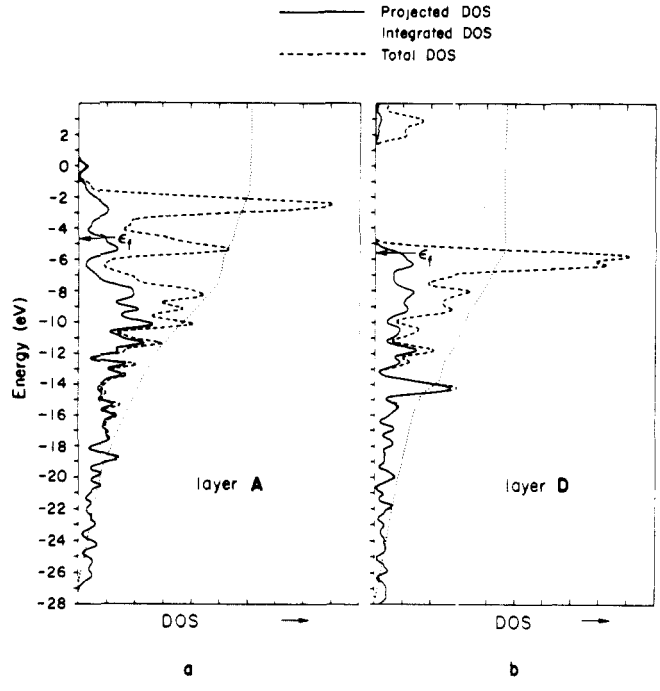

Figure 10. Total density of states (dashed lines) and the B–X bonding states contributions (solid lines) in $B_2X_2^{2-}$ layer A (a) and layer D (b). The element X has a principal quantum number equal to 5.

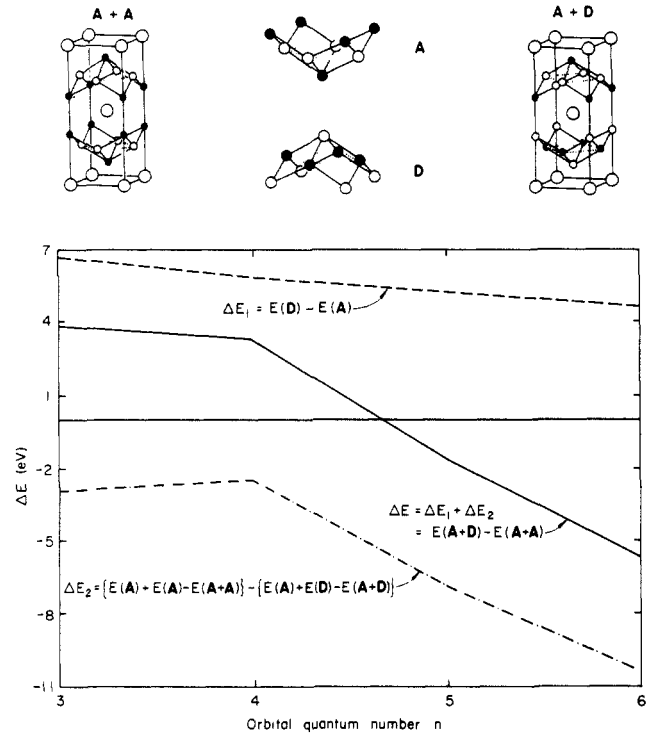

Figure 11. The energy difference between layers D and A (dashed line) and the stabilization energy difference between A + A and A + D stackings (dot-dashed line) as a function of principal quantum number. The sum of these two (solid line) is the total energy difference between A + A and A + D stackings. The $\Delta E = 0$ line separates regions where each 2- or 3-dimensional structure is energetically more stable than the other.

occupied B–X bonding states are reduced from 70% to 54% for layer A due to the site II overlap. For layer D they decrease from 57% to 47%, a smaller reduction. **34** and **35** show the B–X overlap populations for $n = 3$ and 5, respectively. In the $n = 5$ case the overlap populations for both A and D layers are nearly equal, and the energy difference between them is reduced to 5.2 eV. There is also a substantial overlap population developed between Ge's at site II for $n = 5$.

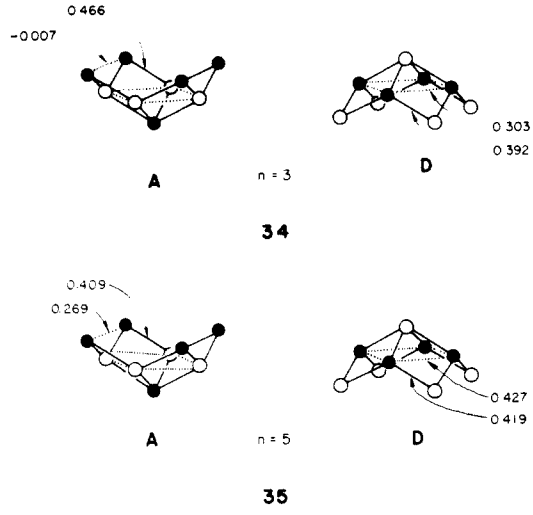

Figure 11 is a plot showing both the energy difference between layers **A** and **D** and the stabilization energy difference between the $ThCr_2Si_2$ and $CaBe_2Ge_2$ structures as a function of the principal quantum number n. The stabilization energy is defined as the difference between the energy sum of the reactant layers and the energy of the composite three-dimensional structure, per unit cell. The energy difference between **A** and **D** favors **A** and the interlayer stabilization energy prefers **A** + **D** stacking. As n increases the **A**, **D** energy difference becomes smaller and the latter factor, the interlayer stacking, wins out. Their sum, the dotted curve, eventually goes into the $CaBe_2Ge_2$ structure region.

Table I lists a selection of some AB_2X_2 compounds adopting the $CaBe_2Ge_2$ structure with ~14 electrons per unit cell.[28] In all these compounds, X has a bigger principal quantum number. An interesting study of the compounds $BaMg_2X_2$ (X = Si, Ge, Sn, Pb) by Eisenmann ann Schäfer[29] shows this trend: As n of the element X increases the structures change gradually from $ThCr_2Si_2$ to $CaBe_2Ge_2$ type, **36**.

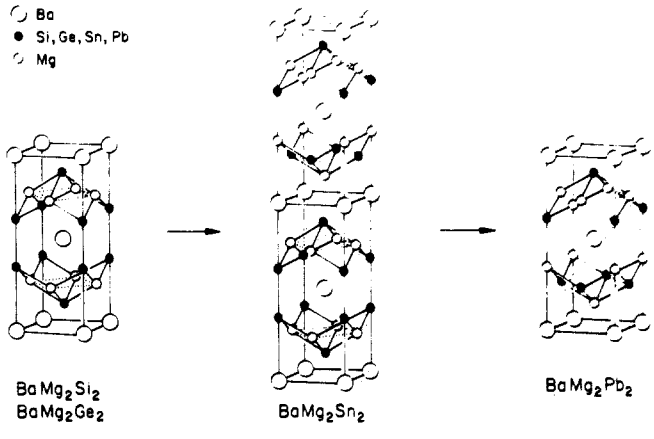

Table I. Some AB_2X_2 Compounds Crystallizing in the $CaBe_2Ge_2$ Structure

AB_2X_2	diff in principal quantum no.[a] $n(X) - n(B)$	diff in electronegativity[b] $\chi(X) - \chi(B)$	no. of electrons per unit cell[c]	ref
$CaBe_2Ge_2$	2	0.4	14	4
$BaZa_2Sn_2$	1	0.3	14	4
$BaMg_2Pb_2$	3	1.0	14	4
$SrCu_2Sb_2$	1	0.2	14	20b
$RELi_2Sb_2$[d]	3	1.1	15	26b
$LaCu_2Sn_2$	1	0.1	13	20e
$CeCu_2Sn_2$	1	0.1	13	27

[a] For s and p electrons. Thus n = 4 for Cu and Zn. [b] Values are from Allred (Allred, A. L. *Inorg. Nucl. Chem.* **1961**, *17*, 215) assuming normal oxidation state. [c] Excluding filled d shell and assuming +3 oxidation state for the rare earth elements. [d] RE = Ce, Pr, Nd.

Table II. Some Transition-Metal AT_2X_2 Compounds Crystallizing in the $CaBe_2Ge_2$ Structure

AT_2X_2	diff in quantum no.[a] $n(X) - n(T)$	diff in electronegativities[b] $\chi(X) - \chi(T)$	no. of electrons per unit cell[c]	ref
$LaIr_2Si_2$	−3	−0.3	29	10
YIr_2Si_2	−3	−0.3	29	11
$LaPt_2Si_2$	−3	−0.4	31	12
YPt_2Si_2	−3	−0.4	31	12
$ThIr_2Si_2$	−3	−0.3	30	12
$ThPt_2Si_2$	−3	−0.4	32	12
UIr_2Si_2	−3	−0.3	32	12
$ThIr_2Ge_2$	−2	−0.2	30	12
$ThPt_2Ge_2$	−2	−0.3	32	12
UIr_2Ge_2	−2	−0.2	32	12
UPt_2Si_2	−3	−0.4	34	30
$HoPt_2Si_2$	−3	−0.4	31	30
$LaPt_2Ge_2$	−2	−0.3	31	31
LnT_2Sb_2[g]	1, 0	0.2, −0.1	33	32
LnT_2Bi_2[g]	2, 1	0.1, −0.2	33	32
APd_2Sb_2[d]	0	−0.1	32–33	33
APd_2Bi_2[d]	1	−0.2	32–33	33
$RERh_2X_2$[e,f]	−2, −1	−0.1, −0.1	31	34
$REIr_2Ge_2$[e]	−2	−0.2	29	35
$SrAu_2Sn_2$	−1	−0.5	32	36
$BaAu_2Sn_2$	−1	−0.3	32	36

[a] s orbital principal quantum numbers are used for transition models. [b] Values are from Allred (Allred, A. L. *Inorg. Nucl. Chem.*, **1961**, *17*, 215) assuming normal oxidation state. [c] Including d electrons. Assuming U^{6+}, Th^{4+}, and all the rare earth elements are in a +3 oxidation state. [d] A = alkaline earth or rare earth metal. [e] RE = rare earth. [f] X = P, As. [g] T = Ni, Pd.

There are quite a few AB_2X_2 compounds crystallizing in the $CaBe_2Ge_2$ structure where B is a transition metal; Table II lists a selection. Some of these exhibit polymorphism, the high-temperature phase being the $CaBe_2Ge_2$ phase. Most of the compounds in Table II have a 29–32 electrons per unit cell, or 9–12 electrons excluding the filled d shell. Thus they have fewer s,p electrons than do the compounds in Table I. Another striking feature is that the X element in Table II is more electropositive in most of the cases. But when the X element is more electropositive its principal quantum number is more likely to be smaller than that of the T element. The structural determinations for most of the compounds in Table II were based on powder patterns. It would be interesting to see the single-crystal structures, since it is not unlikely that the transition metal will play the role of a more electronegative element, as Zn does in $CaZn_2Al_2$.[37] There Zn is more electronegative and has a bigger principal quantum number. It sits at site II (see **9**). In the $CaBe_2Ge_2$ structure, it is still possible to distinguish the roles each element plays, since layers **A** and **D** are not exactly the inverse of each other and Be–Ge is shorter in **D**.

Hofmann and Jeitschko[33] have studied a series of compounds of the stoichiometry MPd_2Pn_2, M = alkaline earth or rare earth,

(28) We count only s and p electrons.
(29) Eisenmann, B.; Schäfer, H. *Z. Anorg. Allg. Chem.* **1974**, 403, 163–172.
(30) Leciejewicz, J.; Szytuła, A.; Ślaski, M.; Zygmunt, A. *Solid State Commun.* **1984**, *52*, 475–478.
(31) Hull, G. W.; Wenick, J. H.; Geballe, T. H.; Waszczak, J. V.; Bernardini, J. E. *Phys. Rev. B* **1981**, *24*, 6715.
(32) Hofmann, W.; Jeitschko, W. *Studies in Inorg. Chemistry*, Vol. 3. *Solid State Chemistry*, 1982. Proceedings of the second European Conference, Veldhoven, The Netherlands, June 7–9, 1982, Metselaar, R., Heijligers, H. J. M., and Schoonman, J., Eds.; Elsevier: Amsterdam, 1983.
(33) Hofmann, W. K.; Jeitschko, W. *Monatsh. Chem.*, in print.
(34) Madar, R.; Chaudonet, P.; Boursier, D.; Senateur, J. P.; Lambert, B., to be published.
(35) Venturini, G.; Méot, M.; Francois, M.; Malaman, B.; Maréché, J. F.; McRae, E.; Roques, B., to be published.
(36) May, N. *Dissertation*, 1974, T. H. Darmstadt.
(37) Cordier, G.; Czech, E.; Schäfer, H. *Z. Naturforsch., B: Anorg. Chem., Org. Chem.* **1984**, *39*, 1629–1632.

Table III. Extended-Hückel Parameters

orbital		H_{ii} (eV)	ζ
Be	2s	-10.0	1.2
	2p	-6.0	1.2
Si (Ge)	3s	-17.3	1.38
	3p	-9.2	1.38
Ca	4s	-7.0	1.2
	4p	-4.0	1.2

Pn = As, Sb, Bi. As Pn goes from As to Bi, the structure changes from the $ThCr_2Si_2$ to the $CaBe_2Ge_2$ type. They argued that this is due to the decreasing Pd-Pd bonding and increasing Pd-pnictogen bonding as the pnictogen size increases. In our main group element case, however, there is no evident Be-Be bonding. Firstly, the Be···Be at site I (**9**) in $CaBe_2Ge_2$ is 2.84 Å, greater than the sum of covalent radii 2.50 Å. Secondly, the occupied states are mostly Ge (>80%) and the empty Be states do not contribute to Be···Be bonding. Were it not for the interlayer interaction, the site occupation would invert in all the layers when Be···Be bonding decreases, as happens in $CaAl_2Zn_2$. We would have the formal oxidation states $Ca^{2+}(Be^{2+})_2(Si^{3-})_2$; the Be^{2+} would be ionic and repulsive to each other and no Be-Be bond would be present.

Acknowledgment. This research was supported by the National Science Foundation through Grant CHE 8406119 and Grant DMR 821722702 to the Materials Science Center at Cornell University. C.Z. would like to thank Professor H. Schäfer and Dr. B. Eisenmann of T. H. Darmstadt for stimulating discussions. We are grateful to J. Burdett and the reviewers for helpful comments, to Cora Eckenroth for the typing, and the Jane Jorgensen and Elisabeth Fields for the drawings.

Appendix

The extended-Hückel method[38] was used in all calculations. Si parameters were used to mimic Ge since no reliable Ge parameters were available. The parameters are assembled in Table III. The geometry was chosen such that Be (Ge) in layer **A** (**D**) is at the center of an ideal Ge_4 (Be_4) tetrahedron. Be-Be (Ge-Ge) = 2.83 Å, Be-Ge = 2.45 Å. A 28K point set[39] was used for the 2-dimensional layer and a 30K point set for the 3-dimensional structure. The calculations were repeated for the 3-dimensional structure with Ca. We found that the calculations with and without Ca were essentially the same.

(38) Hoffmann, R. *J. Chem. Phys.* **1963**, *39*, 1397. Hoffmann, R.; Lipscomb, W. N. *Ibid.*, **1962**, *36*, 2179, 3489; **1962**, *37*, 2872. Ammeter, J. H.; Bürgi, H.-B.; Thibeault, J. C.; Hoffmann, R. *J. Am. Chem. Soc.* **1978**, *100*, 3686.

(39) Pack, J. D.; Monkhorst, H. J. *Phys. Rev. B* **1977**, *16*, 1748.

Tautomeric Instability of 10-Deoxydaunomycinone Hydroquinone[1]

David J. Brand[†] and Jed Fisher*[‡]

Contribution from the Department of Chemistry, University of Minnesota, Minneapolis, Minnesota 55455, and Lipids Research, The Upjohn Company, Kalamazoo, Michigan 49001.
Received August 5, 1985

Abstract: 10-Deoxydaunomycinone and daunomycin are reduced by excess sodium dithionite, under anaerobic conditions, to 10-deoxydaunomycinone hydroquinone. This hydroquinone is not stable, having an approximate rate constant (in 48% MeOH, 52% H_2O, 10 mM Tris-HCl, 10 mM Tris base) for its disappearance of 2×10^{-4} s^{-1}. This disappearance results from a number of tautomeric equilibria, which transform this hydroquinone into more stable species. Typically, eight products in addition to 10-deoxydaunomycinone are detected by reverse-phase liquid chromatographic analysis of the product mixture. Thus far seven of these products have been identified and characterized. Three of the products are diastereomers of (2*R*)-2-acetyl-1,2,3,4,4a,12a-hexahydro-2,6,11-trihydroxy-7-methoxy-5,12-naphthacenedione that have differing stereochemistry at the C-4a,C-12a ring juncture. The major diastereomer (50% of the product) has a trans ring juncture, while the other two diastereomers (13% and 5% of the product) both have a cis ring juncture. Two of the products formed, (2*R*)-2-acetyl-1,2,3,4-tetrahydro-2,11-dihydroxy-7-methoxy-5,12-naphthacenedione (4% of the product) and (2*R*)-2-acetyl-1,2,3,4-tetrahydro-2,6-dihydroxy-7-methoxy-5,12-naphthacenedione (2% of the product), involve the loss of an oxygen from the anthracycline's C ring. The last two products, (8*R*)-8-acetyl-7,9,10,12-tetrahydro-6,8,11-trihydroxy-1-methoxy-5(8*H*)-naphthacenone (11% of the product) and (9*R*)-9-acetyl-7,9,10,12-tetrahydro-6,9,11-trihydroxy-4-methoxy-5(8*H*)-naphthacenone (5% of the product), are derived from the reduction of the dihydroxynaphthacenediones by the excess dithionite present in the mixture. The effect of Fe(III) ion chelation of the anthracycline on the anaerobic dithionite reduction of both daunomycin and 10-deoxydaunomycinone is examined. A modest rate increase for the tautomerization of the hydroquinone is observed for the anaerobic dithionite reduction of the 10-deoxydaunomycinone-Fe(III) chelate, whereas little effect is observed for the daunomycin-Fe(III) chelate. This surprising diversity of materials may account for the abundance of aglycon metabolites found in vivo (many as yet uncharacterized), may prove of value in the synthetic elaboration of anthracyclinones, and is likely to be representative of the hydroquinone behavior of the *p*-dihydroxyanthracyclinones of the rhodomycinone, isorhodomycinone, and pyrromycinone families.

Daunomycin (**1a**) and adriamycin (**1b**) are among the most useful of the antitumor antibiotics.[3] Nevertheless the discovery of the chemical attributes of these molecules responsible for their antibiotic efficacy has proven an extraordinarily difficult problem. Several theories of surprising dissimilarity remain at this time, all of which have experimental evidence in their support.[3,4] The focus of one of these theories[5] centers on the ability of these molecules to enter into redox chemistry by virtue of their quinone moiety. In the presence of a suitable redox enzyme (generally

[†] University of Minnesota.
[‡] The Upjohn Company.

0002-7863/86/1508-3088$01.50/0 © 1986 American Chemical Society